Presented at the DLSU Research Congress 2019
De La Salle University, Manila, Philippines
June 19 to 21, 2019

Design of Modular Casing for Flight Controller and Companion Computer Integration for a Quadcopter UAV

Russel Vince McGrath, Marissa Regalado, Sonny Boy Aniceto Jr, Christer John Ochengco, Alvin Chua
Mechanical Engineering Department, Gokongwei College of Engineering, De La Salle University

Abstract: This paper describes a new modular casing design for a flight controller and companion computer integration on a quadcopter. The absence of protection for a flight controller combined with a companion computer in UAV applications runs the risks of low performance and safety concern of a UAV. In this study, the researchers designed and simulated four different casing designs with the goal of producing the least amount of drag and payload when mounted on the UAV while still sufficiently protecting its internal components. CFD analysis predicted the aerodynamic performance of the four designs. One-way Analysis of Variance (ANOVA) showed that there was no significance on the differences of the four designs in terms of drag. This allowed weighing in other factors in considering the final design through a five-criterion Likert scale. Scores revealed that the hybrid design is the most practical among the four. 3-D printing of the casing with Acrylonitrile Butadiene Styrene (ABS) plastic as the main material was also proposed.

Key Words: UAV; electronic enclosure; aerodynamics; CFD

1. INTRODUCTION

As of the writing, the provided UAV, which is a DJI Flywheel 450 drone, has no casing yet that protects its sensitive parts such as the flight controller, companion computer, etc. With the regulation of flying of UAVs during unfavorable weather conditions, allowing the vehicle to operate with its parts exposed to open air only imposes risk of it getting damaged. Atmospheric conditions such as humidity and temperature and the presence of unwanted airborne particulates, aside from the prospect of damage to the components, can also render it to work inefficiently.

As of writing, the current modular drone being utilized in the university functions completely using a flight controller (i.e. Pixhawk) which allows the drone to be set to have a dedicated flight plan if so desired. However, the computing capability of a flight controller alone limits the possible application of a drone, thus, a companion computer is deemed necessary. The Raspberry Pi (R-Pi) is a small scale computer which possesses high computational capability and can operate in a system such as Linux and/or Android and has ports (USB, ethernet, etc…) just like a typical CPU (Nawrocki, 2016).

Incorporating a computer to a drone opens a lot of possibilities with respect to its applications. This also means that the drone can be programmed accordingly to suit the requirements of the user. An example of this would be obstacle detection and avoidance which uses sensors to understand its surroundings. In a study done by Chee & Zhong (2013), the use of infrared and ultrasonic sensors augmented the capability of a UAV to avoid collision and generate an alternative path. Furthermore, the inclusion of a companion computer allows the usage of a different logic or programming language. For example, Fuzzy Logic which contrary to the traditional Boolean Logic understands values between 0 and 1 (Fuzzy Logic, n.d.). The addition of more sensitive electronic components makes the drone more prone to incurring damages due to natural and man-instigated occurrences thus.

This paper aims to design a protective modular casing for the UAV flight controller and and companion computer in particular using Pixhawk and Raspberry Pi (referred in this paper as R-Pi). The design considered the aerodynamics, payload, and the geometric complexity of the four different design proposals.

2. METHODOLOGY

A. Aerodynamic considerations on UAVs

Aerodynamic forces need be considered in order to control the behavior of an airborne vehicle. The vehicle's weight, motor thrust, and body drag are the forces affecting a quadcopter UAV's flight as in the figure below. The effect of the drag developed at the rotor disks in forward flight can be practically neglected (Bouabdallah, 2007). Gill and D'Andrea (2017) was able to measure this rotor disk drag which was in the order of tenths of a Newton at 10 m/s wind velocity (Gill & D'Andrea, 2017). This tells that most of the drag generated during flight is due to the drone's frame and devices held at its canopy.

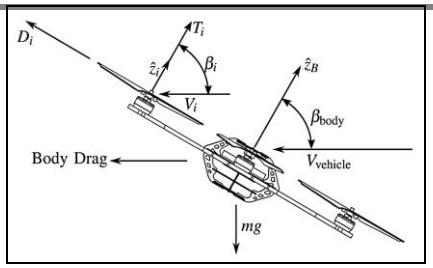

Figure 2.1. Planar view of UAV with forces affecting flight (Gill & D'Andrea, 2017)

Ahmad and Dahalan (2008) were able to show that discretization of a fixed-wing Elang-1 UAV model into various mesh elements at different orders of magnitude does not significantly affect the coefficients of lift and drag resulting from the CFD simulation (Ahmad & Dahalan, 2008).

Also, Gan et al. (2017) was able to show that a droplet-shaped radome patterned after a series of airfoils generates less drag compared when a nacelle-shaped is used (Gan et al., 2017). This radome houses the radar of the heron-type reconnaissance UAV used in the said study. The study reflects the common reputation of airfoils to work favorably in terms of aerodynamics.

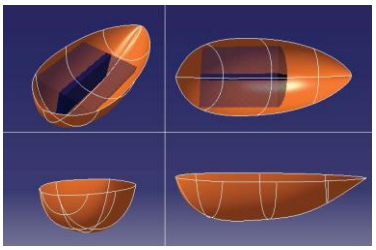

Figure 2.2. Droplet-shaped radome and radar antenna envelope scheme (Gan et al., 2017)

This can be exploited in designing the casing for the drone's Pixhawk and Raspberry Pi microcontroller modules. However, a constraint that needs be considered when using an airfoil is its provision for clearances at a given length. Thus, the stacked height and length of the two components stacked together with clearances for wires and air circulation must be considered.

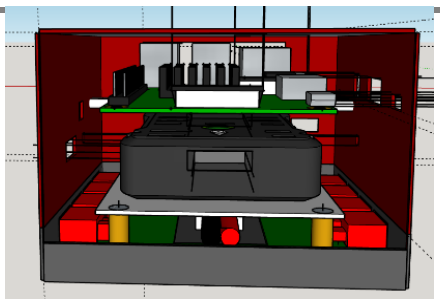

Figure 2.3. Rear view sketch of Pixhawk and Raspberry Pi computer stacked together

B. Materials for electronic casing and enclosure

Electronic enclosures used to be mostly built of metals. However, with the advent of polymers, engineers have been shifting more toward the application of these materials in the design and manufacture of electronic enclosures (Mottahed & Manoochehri, 1999). In recent years, particularly in the design of high-frequency high-density electronic equipment, use of plastics is becoming more common. Plastic materials give obvious advantages of lighter weight, ease of assembly, more aesthetic design options, ease of processing, and cost-effectiveness. The table below summarizes some key points when considering plastics over metals for electronic enclosures.

Table 2.1. Properties of Plastics vs Metals for Electronic Enclosures

Disadvantages of plastic vs metal enclosures	Advantages of plastic vs metal enclosures	Comments
No inherent shielding	Reduced assembly labor	Only high volume
Large tooling investment	Increased fastener options	Few tooling options
Long procurement lead time	Good abrasion resistance	
Raw material and cost availability	Strength to weight ratio; more aesthetic design freedom	
	No corrosion potential	

Resistance to chemical corrosion, resistance to thermal and mechanical shock, flammability, food and drug regulation when used in conjunction with aluminum structure, light weight, machinable, moldable, capable of performance at above a 200°C environment, are some of other important aspects in selecting materials for the electronic applications.

Many enclosures made of metals are used to isolate electrical devices or electronic components from the surrounding to reduce exposure to electromagnetic fields. Some plastic-type shields are coated instead with metallic ink or similar material to serve the same purpose. For this reason, this project study should use plastic in its design since it needs to allow transfer of radio signals between the radio controller and the drone.

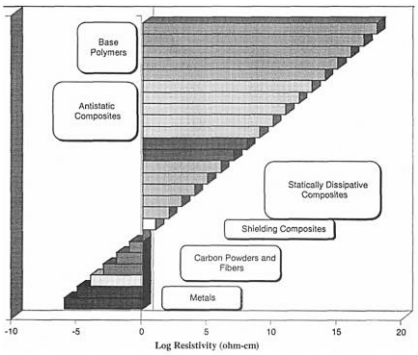

Figure 2.4. Resistivity of materials

Figure 2.4 shows the grouping of materials used in electronic enclosures according to their resistivity. The figure tells that shielding composites or those that can reduce electromagnetic field exposure are among those materials with low resistivity which is related to high conductivity. It is ideal then to use those with higher resistivity values like antistatic composites and base polymers for the purpose of this study.

Table 2.2 gives some properties, particularly mechanical properties, of most common polymers used in electronic enclosures. Modulus of

customized composites not shown in the table can be approximated by the following equations:

$$E_c = V_f E_f + V_m E_m = \left(\frac{1+2nV_f}{1-nV_f}\right)E_m$$

where $$n = \left[\left(\frac{E_f}{E_m}\right)-1\right]\left[\left(\frac{E_f}{E_m}\right)+2\right]^{-1}$$

where E_c, E_f, and E_m are the moduli of the composite, the filler, and the matrix, respectively. V_f and V_m are the volume fractions of the filler and matrix (Dixon & Masi, 1989).

Table 2.2. Mechanical Properties of Some Polymeric Materials

Material	Chemical Resistance	Tensile Strength (ksi)	Density (lb/in^3)	Thermal Conductivity (Btu-ft/h ft^2-F)
Acrylonitrile Butadiene Styrene (ABS)	High to aqueous acids, alkalis, and salt	6.3 to 8.0	0.038	3.2 to 4.8
Acetal	Excellent to moisture, and poor to acids and alkalis	10	0.052	1.56
Acetal – 20% glass	Excellent to moisture, and poor to acids and alkalis	8.5	0.056	1.56
Nylon 6	Resists weak acids, alcohol, and common solvents	5.5 to 13	0.39	1.2
Nylon 6 – 30% glass	Resists weak acids, alcohol, and common solvents	22 to 26	0.05	1.2 to 1.7
Nylon 6/6 – 30% glass	Resists to strong concentration of mineral acids	22 to 26	0.05	1.5
Polycarbonate	Resists weak acids and oils, alkalis and grease	8.5 to 9.0	0.04	1.35 to 1.41
Polycarbonate – 40% glass	Resists weak acids and oils, alkalis and grease	23	0.055	1.53

The four case designs were made using SolidWorksTM as the CAD modelling and simulation platform. The design focused mainly on the idea of resembling an airfoil to minimize the drag, thus, having the least effect on the flight of the drone. The four proposed designs are the following.

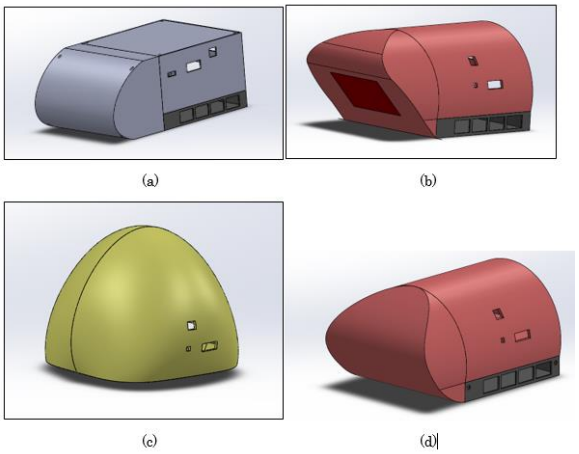

Figure 2.5 CAD models of (a) first design, (b) second design, (c) third design, & (d) fourth design

The first design for the casing of Pixhawk and R-Pi was straightforward such that the space inside is sufficient to fit the components, together with the wirings incorporated with them, hence the rectangular prism. The front panel of this design was based on the tip of an airplane fuselage or that of a radome. The second design introduced more curvature on the body to reduce air turbulence on the sides. This, however, cost the size of the casing since its height needs to compensate for the required clearances. Also, its front panel tried to approximate a triangular cross section to accommodate the prospect of mounting a camera here. The third case design was based on the shape of an egg in its upright position to resemble its aerodynamic streamline geometry. Compared to the first two casings, the third case design did not have any base as it will act as a dome over the components. The aerodynamic behavior of each of the first three designs was simulated using Computational Fluid Dynamics (CFD) through SolidWorks Flow

Simulation. Wind velocities ranging from 0 to 5 m/s with an increment of 0.5 m/s were used to identify the drag and lift coefficients for front and side panel of each design.

3. RESULTS AND DISCUSSION

Drag forces and drag coefficients were obtained in the simulations. These values were plotted and were compared between each design.

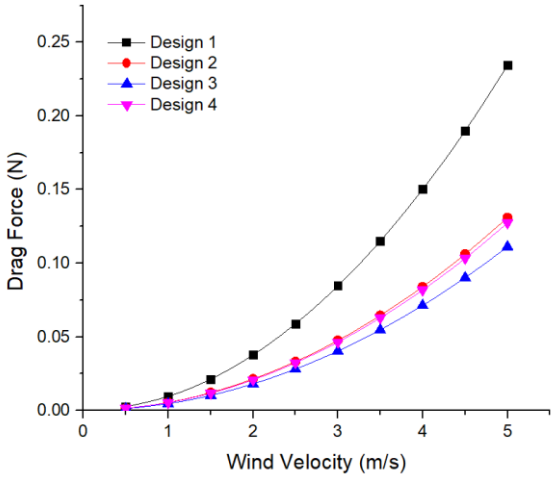

Figure 3.1. Drag due to the side face of case designs at different wind velocities

Figure 3.1. shows the drag forces due to the side face of each case design. Design 1 had the largest amount of drag on the side face because of the rectangular geometry. This forms greater resistance to the momentum of the incoming wind. Since Design 4 is a hybrid design whose side characteristic was derived from Design 2, the two had almost the same drag at their side faces.

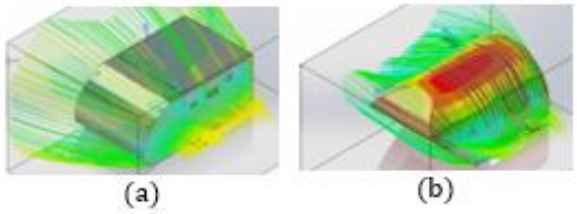

Figure 3.2. (a) Velocity streamline at Side Face of Design 1 and (b) Design 4 Velocity Streamline

Figure 3.2. shows the streamline characteristics of the wind passing through cases 1 and 4 respectively. Simulation results showed that the design of side of case 4 (derived from case 2) is a much favorable path for the incoming wind due to the curved surface which, contrary to case 1, showed to be more streamlined in nature of the shape.

Case 3 resulted to the best aerodynamic characteristic among the four designs. The curved geometry of the side was seen as the key to this. However, the front face performed poorly and had the largest amount of drag. The following graph shows that Design 3 had almost double that of Design 1 in terms of front drag. The large area that the case presented against the wind flow and large curvature resulted in such. This large curvature at the front and back is a result of meeting the required vertical and horizontal clearances due to the two components being housed.

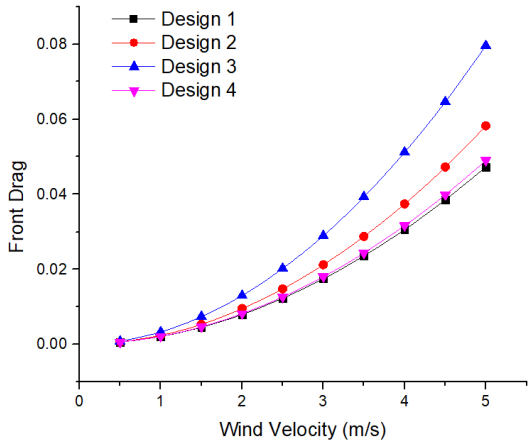

Figure 3.3 Drag due to the front face at different wind velocities

On the other hand, Designs 1 and 4 had almost the same front drag. This, too, was due to the hybrid design of Case 4 resembling the front face characteristics of Case 1. For this reason, Case 4 has overall, the best drag characteristics among others. Combining the side face of Case 2 and front face of Case 1 gave Case 4 an edge in minimizing the resistive force on the drone.

Statistical Analysis

A one-way Analysis of Variance (ANOVA) was performed on the drag forces to determine whether there exist significant differences in their values.

Table 3.1. Analysis of Variance Results for Front and Side Drag

ANOVA Results for Front Drag

Source of Variation	*SS*	*df*	*MS*	*F*	*P-value*	*F crit*
Between Groups	0.000968	3	0.000323	0.772477	0.517025	2.866266
Within Groups	0.015031	36	0.000418			
Total	0.015998	39				

ANOVA Results for Side Drag

Source of Variation	*SS*	*df*	*MS*	*F*	*P-value*	*F crit*
Between Groups	0.014023	3	0.004674	1.594061	0.207773	2.866266
Within Groups	0.105561	36	0.002932			
Total	0.119584	39				

The ANOVA was carried out at $\alpha = 0.05$. For the drag due to the front face of each design, a P-value of 0.68388 was calculated which was higher than the significance level. This corresponded to the calculated F-statistic ($F = 0.7725$) that was lower than the critical value ($F_{crit} = 2.8663$). For the drag due to the side face, a similar tendency was observed. The test recorded a P-value higher than 0.05 and an F lower than the critical value. These indicated that there exists no significant difference in the population means of the front and side drag of all the four designs.

Comparative Analysis

Table 3.2. Likert Chart of Case Comparisons

	Induced Drag		Design Aesthetic	Compactness	Mass	**Total**
	Side	Front				
Case 1	1	4	3	2	3.5	**13.5**
Case 2	2	2	2	4	3.5	**13.5**
Case 3	4	1	1	1	1	**8**
Case 4	3	3	4	3	2	**15**

Table 3.2. shows the weights using Likert scale/chart. The chart was used to better identify which of the designs is of most practical use, considering how they deliver to a particular constraint. Cases 1 and 3 gave extremes for drag characteristics, scoring 1 and 4 alternately in the front and side drag force criteria. Case 4 performed better with a same score of 2. In this part, the maximum drag force (V = 5 m/s) was used as reference for comparison. The design aesthetic, which is rather subjective, was scored by consensus of the researchers giving the highest score to Case 4. The geometry of the base of each design with respect to the platform of the drone was also considered, that is the design's capability to fit just right to the dimensions of the platform. The third design had the most difficulty qualifying in the said criterion because of the nature of the design to extend its curvature to compensate for the clearances required by the components to be contained. Case 4 had the smallest base relative to the other designs which makes it best for this criterion. The payload due to the cases were also obtained using SolidWorks. The software used has the capability to compute the mass of a model with the dimensions and material properties known. Cases 1 and 2 had practically the same mass at around 83 grams. This was followed by Case 4 at 86 grams and then Case 3 with as much as 110 grams.

The result of the weighting system showed that Case 4 design is the most practical design. It scored high across all criteria except for the payload. However, with the slim difference between the masses 83 and 86 grams, it can be said that the chosen design is practically still almost the same in terms of effect in this area.

Temperature Issue of the R-Pi

Further modifications were done on the Case 4 to address the possible temperature that can be reached by the R-Pi which can reach up to 87.6 degrees Celsius when being used presented by the number and significance of computation depending on the application and the duration. For this reason, it was deemed necessary to put a heatsink that will

be able to dissipate the heat produced by the computer. A fan—an active heatsink—was decided to be more appropriate as the computer is enclosed and the usage of fins would be heavier and impractical.

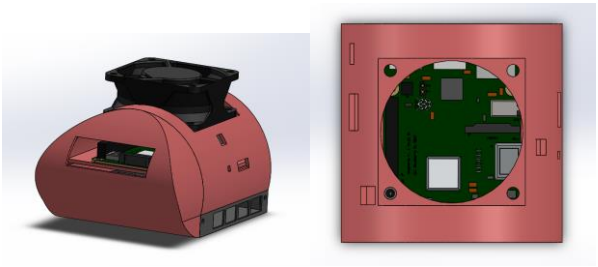

(a) (b)

Figure 3.4. (a) Isometric view of modified case w/ fan (b) top view

Fabrication Simulation of the Case

Previous data gathered led to the decision on the materials to be used on the fabrication of the electronic casing. The base material used was ABS plastic and PVA (Polyvinyl Alcohol) plastic as support. Simulation of the 3D printing was done using Ultimaker Cura 4.0 as the simulation program. The following images show the expected printing outcome for each part of the fabricated case.

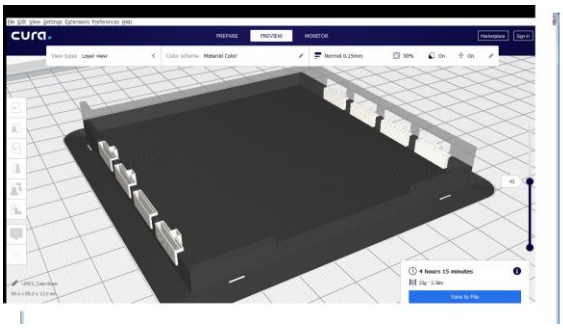

Figure 3.5. Case Base Simulation

The gray regions outlined by white lines require supports; and will be comprised of PVA plastic upon printing completion.

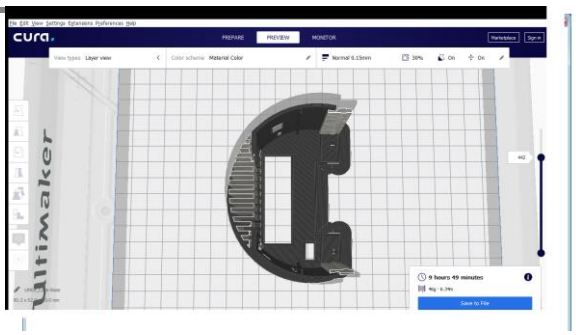

(a)

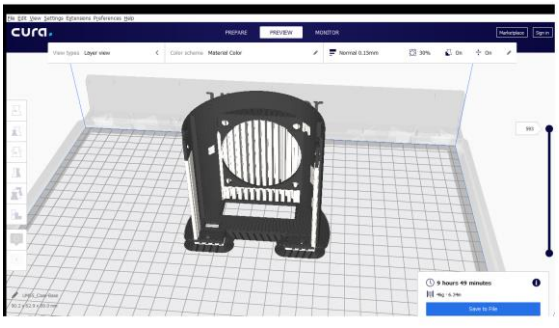

(b)

Figure 3.6. Main Case Simulation: (a) Top View; (b) Isometric View

The main case was oriented in this manner as this was the most optimum in terms of the required supports indicated by the gray regions and white lines.

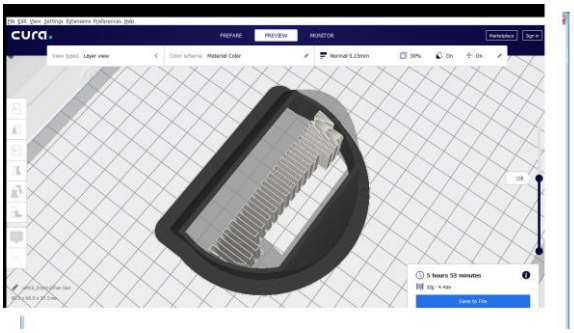

(a)

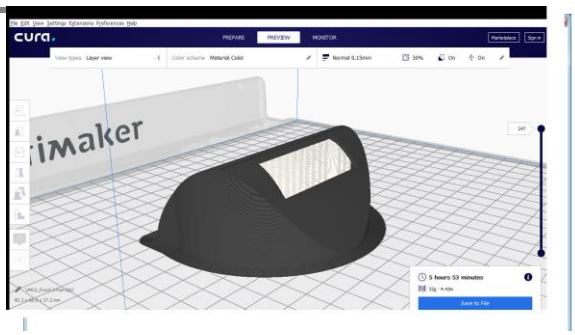

(b)

Figure 3.7. Front Case Simulation: (a) Top View; (b) Isometric View

Comparatively, the front case required more support in the midlle due to the curved profile of the design.

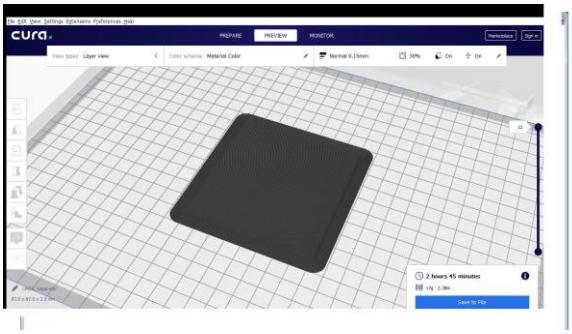

Figure 3.8. Isometric View of the Separator Simulation

The separator was the simplest to print among the case parts and did not require any support.

The supports shown above were automatically placed by the program in the necessary areas indicated by the white lines and gray regions depending on the orientation defined by the user. The above orientations of the case parts were deemed to be the most practical so as to need the least amount of PVA plastic for support purposes. The parts, upon completion of printing, would only need to be soaked in water in order for the PVA supports to disintegrate completely.

4. CONCLUSIONS

The study was concerned with designing a modular casing or canopy that would best fit for the Pixhawk and Raspberry-Pi components of the DJI Flywheel F450 drone. Four designs were proposed and were simulated for aerodynamic performance testing. Drag coefficients were obtained for every design. However, this parameter was identified to not be able to describe the real drag characteristic of each design because of the difference in reference areas inherent to each. Rather, the drag forces calculated in the simulations were used for this reason. A one-way analysis of variance was used to test if there really is significant difference in the heterogeneity and population mean of the drag forces. The ANOVA revealed that there exists no significant difference which allowed the researchers to look on further considerations in choosing the final design. A Likert scale was used to give weights or merits to the four designs according to five criteria namely the side and front drag, design aesthetic, compactness, and design payload. Scores revealed that Case 4 design is the most practical among all. The researchers have decided to use ABS plastic to fabricate the casing as this is relatively the most cost-effective material that was commercially available to acquire.

5. ACKNOWLEDGMENTS

The researchers would like to thank DOST-PCIEERD for funding support. Furthermore, the researchers express their gratitude to the Mechanical Engineering Department of DLSU for supporting the study.

6. REFERENCES

Aerial Work and Operating Limitations for Non-Type Certified Aircraft, 11 C.A.R.§11.11.6.7 (2016). [Portable Document Format File] Taken from www.caap.gov.ph

Bouabdallah, S. (2007). Design and Control of Quadrotors with Application to Autonomous Flying. École Polytechnique Fédérale de Lausanne, La Faculté des Sciences et Techniques de L'Ingénieur, Lausanne.

Chee, K.Y., Zhong, Z.W. (2013). Control, navigation and collision avoidance for an unmanned aerial vehicle. *Sensors and Actuators A: Physical, 190*, 66-76.

Dixon, D., & Masi, J. (1989). Development of composite materials with long-term EMI shielding properties. 3rd International SAMPE Electronic Conference, (pp. 456-467).

Fuzzy Logic. (n.d.). Retrieved July 17, 2018, from TechnoPedia: https://www.techopedia.com/definition/1809/fuzzy-logic

Gan, W., Xiang, J., Ma, T., Zhang, Q., & Bie, D. (2017). Low drag design of radome for unmanned aerial vehicle. 2017 IEEE International Conference on Unmanned Systems (ICUS). IEEE. doi:https://doi.org/10.1109/icus.2017.8278310

Mottahed, B., & Manoochehri, S. (1999). Design Considerations for Electronic Enclosures Utilizing Poylmeric Materials. Polymer-Plastics Technology and Engineering, 883-925. doi:10.1080/03602559909351621

Nawrocki, W. (2016). Measurement Systems and Sensors (2nd Edition) - 2.3 Computer Architecture. Artech House. Retrieved from https://app.knovel.com/hotlink/pdf/id:kt011M0G72/measurement-systems-sensors/computer-architecture